

# UC Davis

## UC Davis Previously Published Works

### Title

Microtubule-associated proteins and motors required for ectopic microtubule array formation in *Saccharomyces cerevisiae*

### Permalink

<https://escholarship.org/uc/item/3qw0j2gh>

### Journal

Genetics, 218(2)

### ISSN

0016-6731

### Authors

King, Brianna R

Meehl, Janet B

Vojnar, Tamira

et al.

### Publication Date


2021-06-24

### DOI

10.1093/genetics/iyab050

Peer reviewed

# Microtubule-associated proteins and motors required for ectopic microtubule array formation in *Saccharomyces cerevisiae*

Brianna R. King <sup>1</sup>, Janet B. Meehl,<sup>2</sup> Tamira Vojnar,<sup>1</sup> Mark Winey,<sup>3</sup> Eric G. Muller,<sup>1</sup> and Trisha N. Davis<sup>1,\*</sup>

<sup>1</sup>Department of Biochemistry, University of Washington, Seattle, WA 98195, USA

<sup>2</sup>Department of Molecular Cellular and Developmental Biology, University of Colorado, Boulder, CO 80309, USA

<sup>3</sup>Department of Molecular and Cellular Biology, University of California, Davis, CA 95616, USA

\*Corresponding author: Department of Biochemistry, University of Washington, UW Box 357350, 1705 NE Pacific Street, Seattle, WA 98195, USA. tdavis@uw.edu

## Abstract

The mitotic spindle is resilient to perturbation due to the concerted, and sometimes redundant, action of motors and microtubule-associated proteins. Here, we utilize an inducible ectopic microtubule nucleation site in the nucleus of *Saccharomyces cerevisiae* to study three necessary steps in the formation of a bipolar array: the recruitment of the  $\gamma$ -tubulin complex, nucleation and elongation of microtubules (MTs), and the organization of MTs relative to each other. This novel tool, an Spc110 chimera, reveals previously unreported roles of the microtubule-associated proteins Stu2, Bim1, and Bik1, and the motors Vik1 and Kip3. We report that Stu2 and Bim1 are required for nucleation and that Bik1 and Kip3 promote nucleation at the ectopic site. Stu2, Bim1, and Kip3 join their homologs XMAP215, EB1 and kinesin-8 as promoters of microtubule nucleation, while Bik1 promotes MT nucleation indirectly via its role in SPB positioning. Furthermore, we find that the nucleation activity of Stu2 *in vivo* correlates with its polymerase activity *in vitro*. Finally, we provide the first evidence that Vik1, a subunit of Kar3/Vik1 kinesin-14, promotes microtubule minus end focusing at the ectopic site.

**Keywords:** microtubule nucleation; microtubule organization; microtubule associated; proteins; motors

## Introduction

High fidelity distribution of genetic material during mitosis requires a dramatic reorganization of microtubules (MTs): The transition from the radiating network of MTs during interphase to the tightly localized bipolar spindle. To form this ordered mitotic array, nucleation of new MTs must be initiated and controlled, and existing MTs must be re-organized.

Successful spindle assembly requires the concerted action of MT organizing centers (MTOCs), motors, and MT associated proteins (MAPs). MTOCs define the distal ends of the spindle and position the spindle in the cell. Motors and MAPs, on the other hand, bind to the MT lattice and have a large variety of functions, from regulating the dynamic instability of MTs to facilitating MT transport.

Several factors complicate our understanding of the roles that MAPs play. First, MAPs act en masse on the multi-micrometer long spindle; many copies of a single protein or a protein complex work together to perform their function efficiently (Page et al. 1994; Geiser et al. 1997; Miller et al. 1998, 2000; Derr et al. 2012; Furuta et al. 2013). Second, MAPs can function either redundantly (Hoyt et al. 1992; Roof et al. 1992; O'Connell et al. 1993; DeZwaan et al. 1997; Cottingham et al. 1999) or antagonistically (O'Connell et al. 1993; Saunders et al. 1997). The concerted MAP interactions result in a bipolar spindle that is resilient to perturbation. While this resiliency is advantageous for life, the interplay among MAPs makes

assigning roles to individual MAPs difficult. Therefore, we utilized a tool that promotes MT array formation at a site that is ectopic to the bipolar spindle—an inducible Spc110 chimera [Spc110c(T)] (Figure 1). Spc110 is a key component of the yeast spindle pole body (SPB) that recruits the conserved  $\gamma$ -tubulin complex to the poles. Using the chimera-based assay, we have measured the contribution of five highly conserved families of MAPs and motors to MT array nucleation and organization. The tumor-overexpressed gene (TOG) polymerase Stu2, the end-binding (EB) protein Bim1, the CLIP170 homolog Bik1, and the kinesin-8 and kinesin-14 motor proteins, Kip3 and Vik1, were examined. Each have been previously implicated in MT nucleation and spindle assembly.

*Saccharomyces cerevisiae* has a closed mitosis, and nucleation of new MTs during spindle assembly is narrowly localized to the nuclear face of the SPB. Of the five candidate budding yeast proteins, four have homologs that are implicated in MT nucleation in other organisms. Though these proteins primarily bind the MT lattice, four interact with components of the SPB: Stu2, Bim1, Bik1, and Vik1 (Wigge et al. 1998; Manning et al. 1999; Newman et al. 2000; Usui et al. 2003; Wang et al. 2012). Furthermore, homologs of Stu2, Bim1, and Kip3 were shown to promote MT nucleation both *in vivo* and *in vitro* (Popov et al. 2002; Vitre et al. 2008; West and McIntosh 2008; Erent et al. 2012; Wiczorek et al. 2015; Thawani et al. 2018; King et al. 2020), and Stu2 specifically promotes cytoplasmic MT nucleation (Gunzelmann et al. 2018).

Received: January 08, 2021. Accepted: March 04, 2021

© The Author(s) 2021. Published by Oxford University Press on behalf of Genetics Society of America. All rights reserved.

For permissions, please email: journals.permissions@oup.com

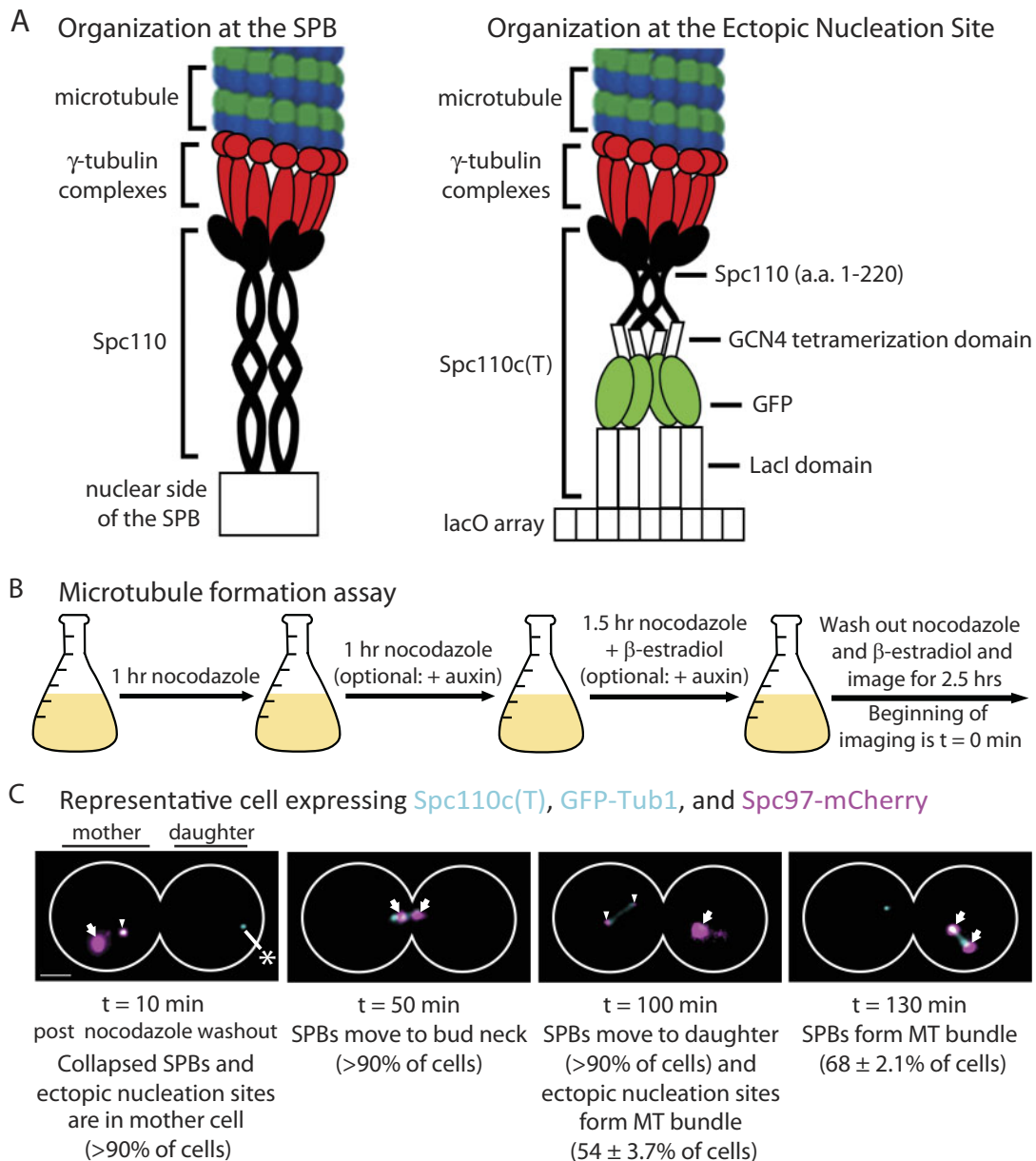


**Figure 1** The  $\gamma$ -tubulin complex serves as a robust MT nucleation template at the wild-type SPB and the *Spc110c(T)*. (A) (Left) Full-length *Spc110* dimerizes via a coiled coil domain and anchors  $\gamma$ -tubulin complexes to the nuclear side of the budding yeast SPB. (Right) The *Spc110c(T)* is comprised of the N-terminal 220 amino acids of *Spc110*, a tetramerization version of the GCN4 domain, a GFP tag, and a lac repressor domain which binds *lacO* arrays integrated into Chromosome XII. (B) Diagram of the *Spc110c(T)* MT formation assay. (C) A representative timeline of events following nocodazole arrest,  $\beta$ -estradiol pulse induction of *Spc110c(T)*, and nocodazole release (RKY52). At the earliest timepoints, SPBs are collapsed and the *Spc110c(T)* is colocalized with *Spc97-mCherry*. SPBs then move to the bud neck and into the daughter cell in  $92 \pm 4.6\%$  of cells. Following SPB movement to daughter, the *Spc110c(T)* forms MT arrays in the mother and the SPBs form spindles.  $\gamma$ -tubulin complexes are visualized using expression of *Spc97-mCherry* (shown in magenta), and  $\alpha\beta$ -tubulin is visualized using expression of *GFP-Tub1* (shown in cyan). Arrows denote SPBs and carets denote ectopically localized  $\gamma$ -tubulin complexes. Asterisk in left panel denotes a commonly observed phenomenon following *Spc110c(T)* expression—large GFP puncta in daughter cell that do not recruit *Spc97-mCherry* believed to be inactive aggregates. Scale bar is 2  $\mu$ M.

Conversely, Plk1, the fission yeast kinesin-14 motor, suppresses MT nucleation (Olmsted et al. 2014).

Spindle assembly also requires careful regulation of dynamic instability at the MT plus ends, which extend away from the SPB and connect to the kinetochores. In the case of *Stu2*, *Bim1*, and *Bik1*, there is evidence that each one stabilizes MTs. *Stu2* is a member of the XMAP215 family of MT polymerases that promote growth rates (Brouhard et al. 2008). *Bim1* inhibits catastrophe and does so in complex with *Bik1* (Blake-Hodek et al. 2010). *Kip3*, on the other hand, destabilizes long MTs and stabilizes short MTs (Gupta et al. 2006;

Varga et al. 2006; Tischer et al. 2009; Gardner et al. 2011; Reese et al. 2011; Su et al. 2011; Melbinger et al. 2012; Fukuda et al. 2014).

In addition to regulating the length of MTs, MAPs or motors can function to organize MTs relative to each other. Specifically, interpolar MTs are organized to overlap in the midzone, while kinetochore MTs are focused toward MTOCs via their minus ends in order to generate tension. Dynein and kinesin-14 motors promote MT minus end focusing at the MTOCs in *Drosophila melanogaster* and *Homo sapiens* (Endow and Komma 1998; Kwon et al. 2008; Lecland and Lüders 2014). No such activity has been

reported in budding yeast; however, mutations to SPC110 that weaken the nuclear SPB-MT interface are synthetically lethal with deletion of KAR3 or VIK1 (of the Kar3Vik1 complex) (Greenland et al. 2010) and BIM1 (Costanzo et al. 2016).

## Materials and methods

### Media

YPD was prepared as described (Burke et al. 2000). YPD 3x ADE media is YPD with 15 mg/ml adenine. LoFlo S liquid medium contains 1.93 g/l yeast nitrogen base LoFlo (Formedium™) plus 5 g/l ammonium sulfate. LoFlo SD<sup>+</sup> medium is LoFlo S medium with 2% glucose and 1/100 dilution of a filter sterilized solution of L-amino acids and nutrients containing 0.2% arginine, histidine and methionine, 0.3% isoleucine, leucine, and lysine, 0.4% tryptophan, 0.5% phenylalanine and threonine, 0.25% uracil and 1.5% adenine. The high concentration of adenine suppressed the formation of red fluorescent pigment in our *ade2*, *ADE3* strains.

### Strain construction

All strains used in this study are derivatives of W303 (Thomas and Rothstein 1989) (Supplementary Table S1). Transformations were performed by a standard lithium acetate method (Gietz et al. 1995). The tetrameric Spc110 chimera construct, Spc110c(T), consisting of SPC110(1-220a.a.)-GCN4-GFP-lacI was integrated at ADE2 with a promoter specific to the transcription factor Z<sub>4</sub>EV as previously described (Lyon et al. 2016). Z<sub>4</sub>EV was integrated at CAN1 with a  $\beta$ -estradiol inducible promoter (Mcisaac et al.). Two hundred and fifty-six copies of a lacO repeat were integrated into chromosome XII as described previously (Lyon et al. 2016). Briefly, pGM22 was cut once using NcoI to integrate the full plasmid in the intergenic region between TRX1 and PDC1 at coordinate 232294. MAPs were C-terminally tagged with 3 V5 epitopes and the auxin-responsive protein IAA7 (Shetty et al. 2019). The ubiquitin ligase complex protein OsTIR1, necessary for auxin-inducible degradation, was integrated at LEU2. Spc97 was C-terminally tagged with mCherry. GFP-Tub1 under the TUB1 promoter was integrated at URA3 using pAFS125 (Straight et al. 1997).

### Electron tomography

TVY11-123D was incubated with 1 mM auxin (Millipore Sigma, St. Louis, MO, USA) for 2.5 hours (Spc110-AID degradation greater than 90%). Cells were collected on a Millipore filter by vacuum filtration and high pressure frozen using a Wohlwend Compact 02 high-pressure freezer (Technotrade International, Manchester, New Hampshire, USA). Cells were freeze substituted at low temperature in acetone containing 0.25% glutaraldehyde and 0.1% uranyl acetate, then infiltrated with Lowicryl HM20 resin. After polymerization, 350 nm serial sections were collected on copper slot grids coated with formvar, post-stained with 2% aqueous uranyl acetate and Reynold's lead citrate. Tilt series were collected on a Technai F30 microscope. Tomograms were computed and modeled using the IMOD software package (RRID: SCR\_003297) (Kremer et al. 1996; Mastronarde 1997; O'Toole et al. 2002).

### $\gamma$ -tubulin complex recruitment assay

Cells were grown asynchronously in YPD 3xADE at 25°C to 40 Klett units, within log phase. Cells were first pulsed with 0.1  $\mu$ M  $\beta$ -estradiol (Millipore Sigma) for 10 minutes and then washed with YPD 3xADE. Cells were then treated with 15  $\mu$ g/ml nocodazole (Millipore Sigma) for 2.5 hours. In cells harboring a protein tagged with auxin-inducible degron (AID), cells were simultaneously treated with 1 mM auxin (Millipore Sigma) during the

2.5 hours incubation. Cells were pelleted and resuspended in 100  $\mu$ l of LoFlo SD medium, placed on Lo-Flo SD + 1% agarose pad (SeaKem® Gold Agarose, Lonza, Rockland, ME, USA) supplemented with 15  $\mu$ g/ml nocodazole and 1 mM auxin, as previously described (Muller et al., 2005) (<https://www.youtube.com/watch?v=ZrZVbFg9NE8>). Cells were imaged using either a DeltaVision system (Applied Precision, Issaquah, WA, USA) or, in the case of *vik1 $\Delta$ /vik1 $\Delta$*  cells, an Axio Observer (Carl Zeiss). The DeltaVision system was equipped with IX70 inverted microscope (Olympus, Center Valley, PA, USA), a Coolsnap HQ digital camera (Photometrics, Tucson, AZ, USA), and a U Plan Apo 100X objective (1.35 NA). The inverted Axio Observer was equipped with an ORCA-Flash4.0 V3 Digital CMOS camera (Hamamatsu), a Spectra X LED light engine (Lumencor), a Plan-APOCHROMAT 63X/1.46 objective (Zeiss), and a 432/523/702 nm BrightLine® triple-band bandpass filter (Semrock, Inc., Rochester, NY, USA).

For the recruitment assay, the Spc110c(T) was visualized using its integrated GFP fluorescence and  $\gamma$ -tubulin complexes were visualized with Spc97-mCherry. GFP was imaged with 0.25 seconds exposures, mCherry was imaged with 0.4 seconds exposures, and 25 0.2  $\mu$ m z-sections were taken. Images taken on the DeltaVision microscope were binned 2  $\times$  2, while images taken on the Axio Observer were not binned.

Recruitment analysis was performed using the Spots colocalization function of Imaris software (Bitplane, Switzerland) (RRID: SCR\_007370). Spc110(1-220a.a.)-GCN4-GFP-lacI puncta were located by assigning an XY diameter of 0.4  $\mu$ m and a Z diameter of 1.3  $\mu$ m. Spc97-mCherry puncta were located by assigning an XY diameter of 0.4  $\mu$ m and a Z diameter of 1.8  $\mu$ m. Quality of spots was manually determined. To exclude background fluorescence of the agarose pad in the total number of puncta, GFP and mCherry fluorescent puncta were first colocalized to be within 4  $\mu$ m. These filtered spots were then colocalized within 0.5  $\mu$ m and reported as the percent of Spc110c(T) puncta with recruitment events.

Spc97-mCherry intensity analysis was performed using the intensity sum of mCherry fluorescent puncta that colocalized within 0.5  $\mu$ m of GFP fluorescent puncta. Recruitment experiments with a strain carrying *vik1 $\Delta$ /vik1 $\Delta$*  and a control strain were performed using the Zeiss Axio Observer, resulting in different absolute values from the other MAPs and motors recruitment experiments.

### MT formation assay

Cells were grown asynchronously in YPD 3xADE at 25°C to 40 Klett units, within log phase. Cells were then treated with 15  $\mu$ g/ml nocodazole for 2 hours. In cells harboring a protein tagged with AID, cells were simultaneously treated with 1 mM auxin for the second hour. 0.1  $\mu$ M  $\beta$ -estradiol was then added, and the incubation continued for an additional 1.5 hours. Cells were released from nocodazole and  $\beta$ -estradiol and released into YPD 3xADE for 10 minutes (in cells harboring a protein tagged with AID, cells were incubated with 1 mM auxin). Cells were pelleted and placed on Lo-Flo agarose pads (in cells harboring a protein tagged with AID, agarose was supplemented with auxin). Cells were imaged at 10-minute intervals for 2.5 hours as described above for the  $\gamma$ -tubulin recruitment assay.

For the MT formation assay, the Spc110c(T) and Spc97-mCherry were visualized and acquired as described for the recruitment assay, with MTs visualized using GFP-Tub1 and 15 0.2  $\mu$ m z-sections.

MT formation and persistence analysis was performed manually using Imaris software (Bitplane).

## Calculations for an indirect effect of Bik1

In control cells where SPBs move to the daughter, the fraction of those cells that form Spc110c(T)-associated MT arrays, or  $A_{\text{daughter}}$ , is 0.58. When SPBs remain in the mother, the fraction, or  $A_{\text{mother}}$ , is 0.083. When Bik1-AID is degraded, the fraction of cells with SPBs remaining in the mother, or  $SPB_{\text{mother}}$ , is 0.95, while the fraction of cells with SPBs moving to the daughter, or  $SPB_{\text{daughter}}$ , is 0.048. If the effect of Bik1-AID on ectopic MT array formation is due purely to SPB localization, the predicted fraction of cells with Spc110c(T)-associated MT arrays is 0.11, as given by the following equation:

$$\text{Predicted total fraction} = SPB_{\text{daughter}} \times A_{\text{daughter}} + SPB_{\text{mother}} \times A_{\text{mother}}$$

## Line scan analysis

Ten-pixel wide lines along Spc110c(T)-associated MT arrays were drawn manually using ImageJ (National Institutes of Health, USA), and measured values were the average fluorescence intensity at each point on the line scan. Background fluorescence was calculated using the average of the last five points of the line scan. After subtraction of background, line scans were analyzed using the peakfinder and trapz functions of Matlab (MathWorks, USA).

## Data availability

Strains and plasmids used in this study are available upon request (Supplementary Tables S1 and S2). The authors affirm that all data necessary confirming the conclusions of the article are present within the article, figures, tables, and supplemental information. Supplementary material is available at figshare: <https://doi.org/10.25386/genetics.14120393>.

## Results and discussion

### Spc110c(T) recruits the $\gamma$ -tubulin complex and forms MT arrays in vivo

The Spc110c(T) is a  $\beta$ -estradiol inducible chimeric protein comprised of the N-terminal 220 amino acids of Spc110, a tetramerization version of the GCN4 domain, a GFP tag, and a lac repressor domain. When Spc110c(T) expression is induced during nocodazole treatment to depolymerize MTs, the Spc110c(T) recruits the  $\gamma$ -tubulin complex to the DNA, rather than the SPB, through lac operator/lac repressor interactions (Figure 1, A and B, Supplementary Movie S1, Materials and Methods). This provides an ectopic site of MT nucleation when released from nocodazole arrest. Over a three-hour period,  $68 \pm 2.1\%$  cells form MT arrays at the SPB, while  $54 \pm 3.7\%$  of cells form ectopic MT arrays at the Spc110c(T) (Figure 1C). Arrays at the Spc110c(T) are composed of antiparallel MTs with capped minus ends, as revealed by electron tomography (Figure 2). While Spc110c(T)-associated MT bundles are less organized than mitotic spindles, MT minus ends cluster.

### MAPs and motors are not required for localization of $\gamma$ -tubulin complex to the Spc110c(T)

An initial, necessary step in MT nucleation is the recruitment of the  $\gamma$ -tubulin complex to Spc110 at the SPB. When cellular MTs are depolymerized in  $15 \mu\text{M}$  nocodazole, the Spc110c(T) recruits the  $\gamma$ -tubulin complex, which can be quantified as the percent of Spc110c(T) puncta that ectopically colocalize with Spc97-mCherry puncta (Figure 3). As described above, several of the candidate MAPs and motors interact with components of the SPB, so we asked whether the candidate proteins affected the ability of the N-terminus of Spc110 to recruit or bind  $\gamma$ -tubulin complexes. We tested the effects of deletion of VIK1 and KIP3 and the effect of depletion of Stu2, Bim1, and Bik1 using an auxin-degradation system. We found that none of the MAPs or motors affect the percent of Spc110c(T) that recruit the  $\gamma$ -tubulin complex to Spc110c(T) (Figure 3). We then measured the amount of

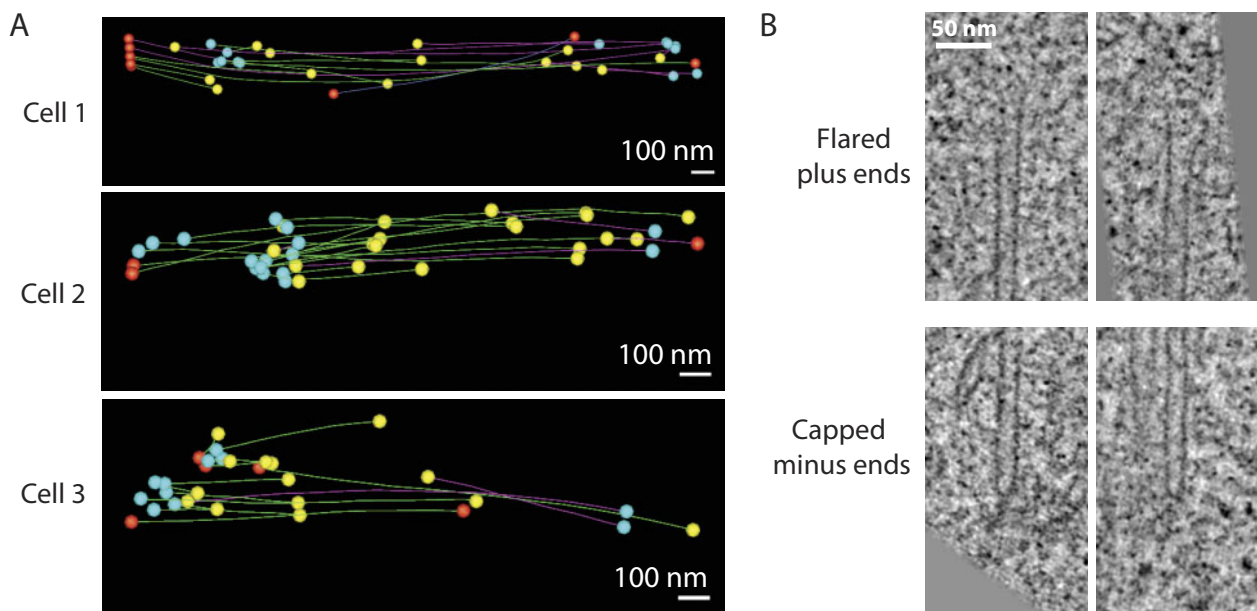


**Figure 2** The Spc110c(T) forms bipolar MT arrays with capped minus ends and flared plus ends. (A) Electron tomography of MT bundles associated with Spc110c(T) revealed antiparallel MTs with clusters of capped minus ends (TVY11-123D). Capped minus ends shown in blue, flared plus ends shown in yellow, and MT ends out of volume shown in orange. Green MTs have minus end left of their plus end, and pink MTs have opposite polarity. Polarity of MTs was assessed by their visible ends. (B) Representative capped minus ends and flared plus ends from electron tomography. Left two panels: The flared end and capped end of a single MT. Right two panels: The flared end and capped end of a second MT.

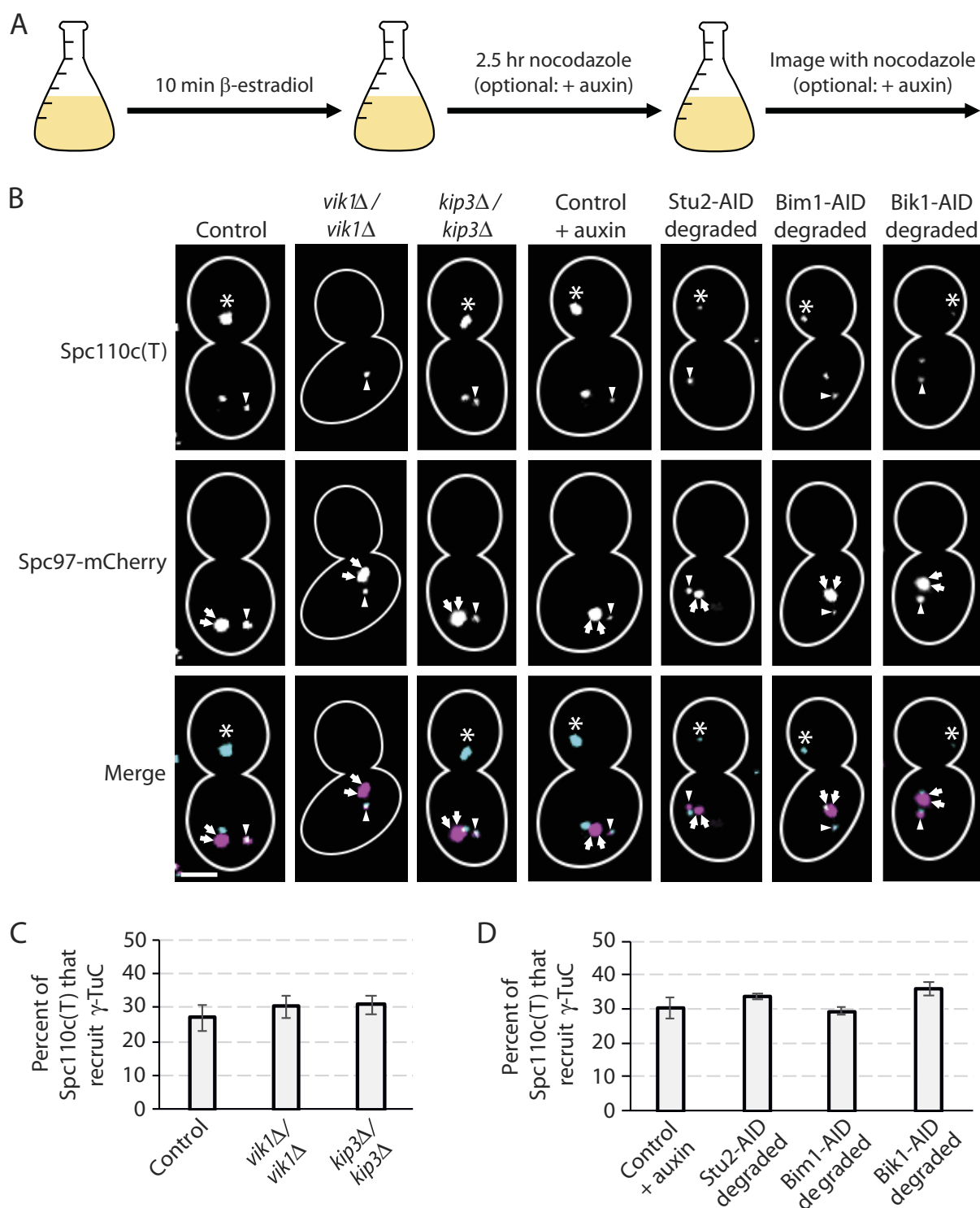


**Figure 3** MAPs and motors are not required for  $\gamma$ -tubulin complex localization to the Spc110c(T). (A) Diagram of the Spc110c(T)  $\gamma$ -tubulin complex recruitment assay. (B) Representative recruitment of  $\gamma$ -tubulin complex to Spc110c(T) in control (RKY44), *vik1Δ/vik1Δ* (RKY174), *kip3Δ/kip3Δ* (RKY56), and auxin-treated control, Stu2-AID (RKY14), Bim1-AID (RKY47), and Bik1-AID (RKY51) cells.  $\gamma$ -tubulin complexes are visualized using expression of Spc97-mCherry (shown in magenta). Arrows denote SPBs and caret symbols denote ectopically localized  $\gamma$ -tubulin complexes. Asterisks denote GFP puncta in daughter cell that do not recruit Spc97-mCherry and are in the cytoplasm. Scale bar is 3  $\mu$ M. (C) Percent of cells in which the Spc110c(T) recruits the  $\gamma$ -tubulin complex is unaffected by deletion of *VIK1* or *KIP3*. Values shown are mean  $\pm$  S.D. There were 2 biological replicates for all conditions and 234, 316, and 375 total cells for control, *vik1Δ/vik1Δ* and *kip3Δ/kip3Δ*, respectively. (D) Percent of cells in which the Spc110c(T) recruits the  $\gamma$ -tubulin complex is unaffected by degradation of Stu2, Bim1, or Bik1. Values shown are mean  $\pm$  S.D. There were 2 biological replicates for all conditions and 249, 389, 248, and 315 total cells for control plus auxin, Stu2-AID degraded, Bim1-AID degraded, and Bik1-AID degraded, respectively.

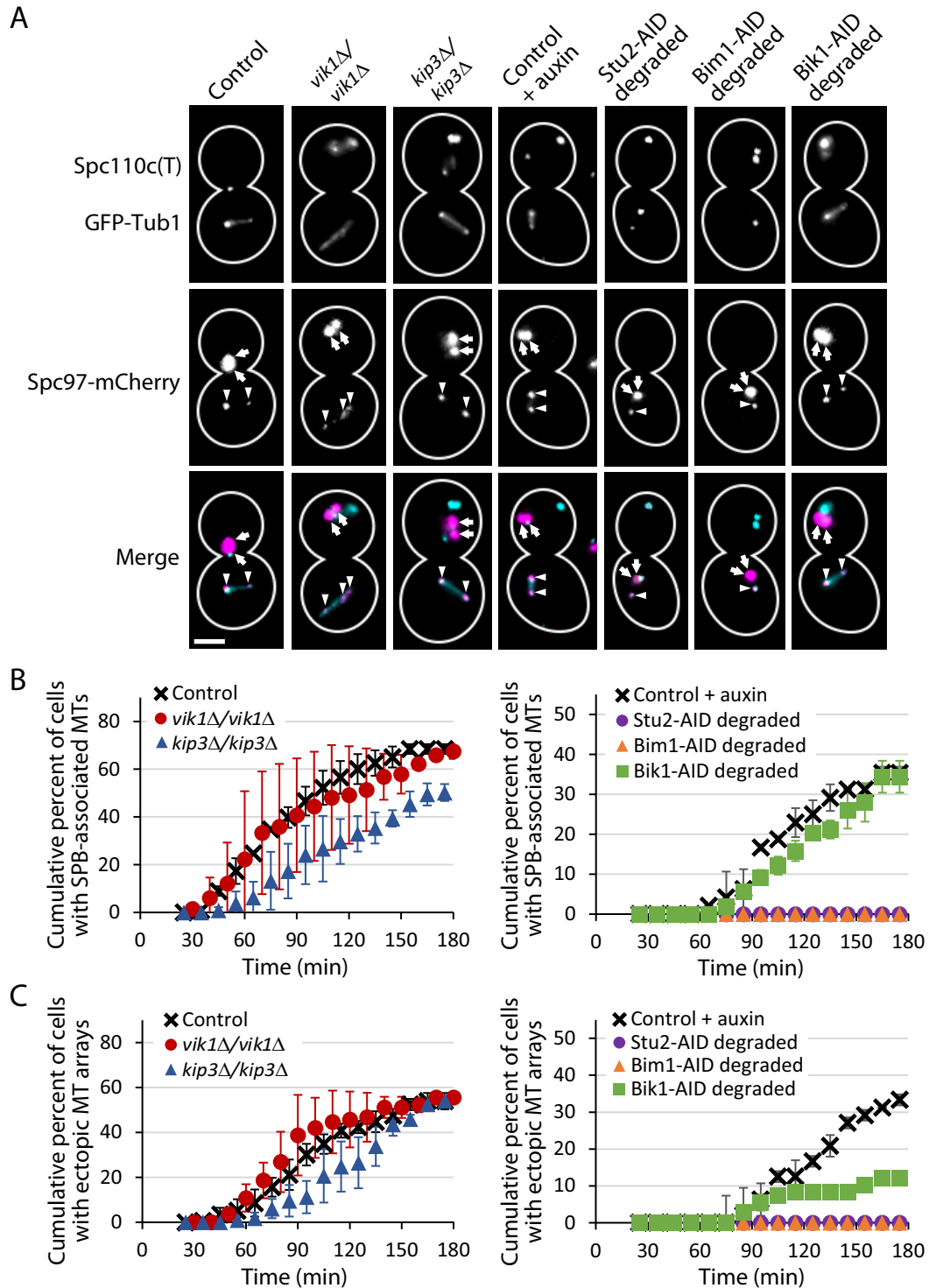


**Figure 4** Stu2, Bim1, Bik1, and Kip3 promote MT array formation from the Spc110c(T). (A) Representative MT array formation from the Spc110c(T) in control (RKY52), *vik1Δ/vik1Δ* (RKY31), *kip3Δ/kip3Δ* (RKY49), and auxin-treated control, Stu2-AID (RKY7), Bim1-AID (RKY46), and Bik1-AID (RKY36) strains.  $\gamma$ -tubulin complexes are visualized with Spc97-mCherry (shown in magenta) and  $\alpha\beta$ -tubulin is visualized with GFP-Tub1 (shown in cyan). Arrows denote SPBs and carets denote ectopically localized  $\gamma$ -tubulin complexes. Asterisks denote GFP puncta in daughter cell that do not recruit Spc97-mCherry believed to be inactive aggregates. Scale bar is 3  $\mu$ M. (B) Cumulative percent of cells over time in which SPBs form spindles. Values shown are mean  $\pm$  S.D. There were  $\geq 2$  biological replicates and 157, 108, 120, 96, 173, 155, and 108 total cells for control, *vik1Δ/vik1Δ*, *kip3Δ/kip3Δ*, control plus auxin, Stu2-AID degraded, Bim1-AID degraded, and Bik1-AID degraded, respectively. (C) Cumulative percent of cells over time in which Spc110c(T)s form MT arrays. Values shown are mean  $\pm$  S.D. Cell populations are the same as in part B.

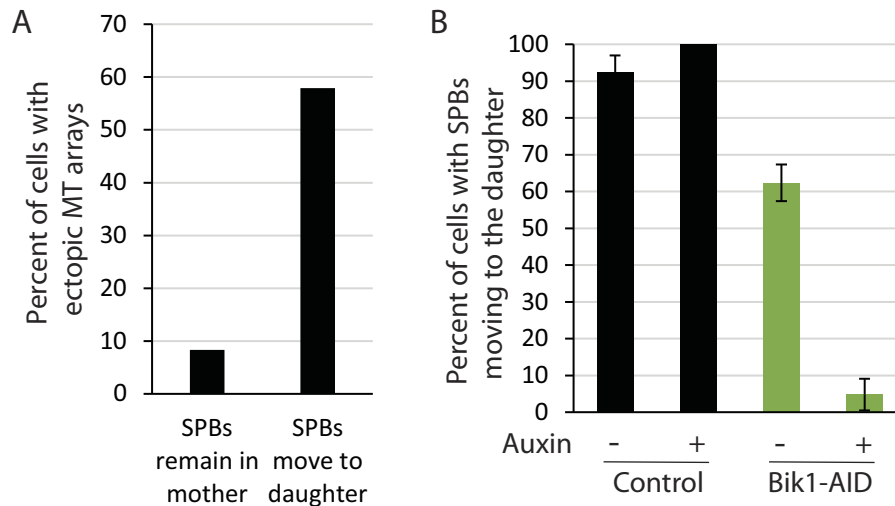


**Figure 5** Bik1 indirectly promotes MT nucleation at the Spc110c(T). (A) SPB movement to daughter cells correlates positively with Spc110c(T) MT formation. During the examination of ectopic MT formation in RKY52, cells were scored for the position of the SPB in the budded cells. (B) Expression of Bik1-AID and depletion of Bik1-AID (RKY36) results in decreased SPB movement to daughter cells. Values shown are mean  $\pm$  S.D. There were  $\geq 2$  biological replicates and 157, 204, 100, and 108 total cells, for control, control plus auxin, Bik1-AID, and Bik1-AID plus auxin, respectively.

Spc97-mCherry recruited to individual Spc110c(T)s and found no difference between control strains and MAP- or motor-deficient strains (Supplementary Figure S1).

### Stu2, Bim1, Bik1, and Kip3 promote MT formation at the Spc110c(T)

Following nocodazole treatment and subsequent release, the Spc110c(T) promotes formation of ectopic MT arrays in  $54 \pm 3.7\%$  of cells, ( $32 \pm 1.5\%$  with auxin treatment) (Figure 4). We tested the role of Vik1, Kip3, Stu2, Bim1, and Bik1 in this process by quantifying the cumulative percent of cells forming MT arrays at both the SPBs and ectopic sites. We found that Vik1 was not required for MT array formation at either the SPB or the Spc110c(T) (Figure 4, B and C). Strikingly, Stu2 and Bim1 are essential for MT formation from both the Spc110c(T) and the SPB. No visible MTs form when either Stu2-AID or Bim1-AID is degraded (78% and 99% degradation, respectively) (Figure 4, B and C).

Although not essential for MT array formation, Kip3 and Bik1 each promote MT array formation at the Spc110c(T). For Kip3, MT formation is slightly delayed in *kip3 $\Delta$ /kip3 $\Delta$*  cells at both the ectopic site and the SPB (Figure 4C).

When Bik1-AID is degraded (82% degradation), MT formation is also delayed at the ectopic site, but by a unique mechanism. While degradation of Bik1-AID does not impact MT array formation between SPBs (Figure 4B), it does largely disrupt the movement of SPBs to the daughter (Figure 5). As seen in control cells, this movement of the SPB to the daughter enhances the formation of the ectopic MT bundle in the mother from 8.3% to 58% (Figure 5A). If the impact of Bik1 degradation on ectopic MT array formation is due to SPB localization, we would expect ectopic MT array formation to be approximately 11% (calculations shown in Materials and Methods). As the observed value is  $12 \pm 0.36\%$ , the reduction of ectopic MT formation following Bik-AID degradation is most likely indirect and largely a result of the effect on SPB positioning. A role for Bik1 in SPB positioning has previously been observed (Carvalho et al. 2004; Caudron et al. 2008; McNally 2013).

To quantify the stability of the Spc110c(T) associated MT arrays, we measured the persistence of the arrays. In strains that

form Spc110c(T) associated MT arrays, we found no difference in array persistence compared to controls (Supplementary Figure S2).

### The ability of the Spc110c(T) to form MT arrays correlates with the polymerase activity of Stu2

Recent work from our lab showed that the MT polymerization rate *in vitro* of XMAP215, the *X. laevis* homolog of Stu2, correlates with its ability to nucleate MTs *in vitro*. We asked whether previously published MT polymerization rates of Stu2 mutants *in vitro* would correlate with their promotion of MT array formation at the Spc110c(T).

Stu2 polymerase activity can be modulated by inhibiting either its ability to bind free tubulin via TOG domains, to localize to the MT lattice via the basic MT binding domain, or to dimerize via the coiled coil domain. One study has quantified the polymerase activity of various Stu2 mutants, placing them into three categories: wild-type polymerase activity, moderate polymerase activity, or no activity (Figure 6A, data from, Geyer et al. 2018).

As shown above, Stu2 is required for MT formation following nocodazole treatment (Figure 4). When Stu2-AID is degraded, MT array formation is rescued through constitutive expression of *STU2* at an exogenous locus (Figure 6). We utilized this system to compare Stu2 mutants with different polymerase activities. Stu2-AID at its native locus was degraded during Spc110c(T) expression, and *stu2* mutants were expressed constitutively at *LEU2*. As hypothesized, Stu2 polymerase activity *in vitro* correlated with MT formation activity (Figure 6, C and D).

### Kinesin-14 motor complex protein Vik1 promotes focusing of MT minus ends

While Vik1 was not required for ectopic recruitment of the  $\gamma$ -tubulin complex to Spc110c(T), nor ectopic MT array formation, deletion of *VIK1* did result in decreased MT minus end clustering within the ectopic microtubule array (Figure 7). We quantified this phenotype by measuring Spc97-mCherry intensity along Spc110c(T)-associated MT arrays (Figure 7B). Importantly, the total Spc97-mCherry intensity along Spc110c(T)-associated MT



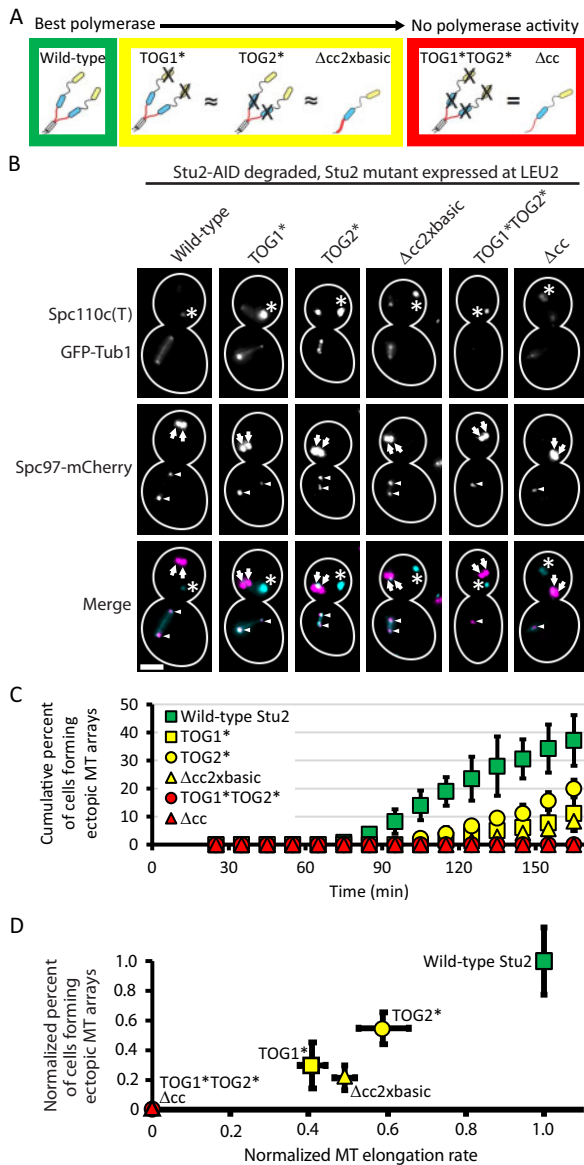


**Figure 6** Stu2 promotion of MT nucleation at the Spc110c(T) correlates with its reported polymerase activity *in vitro*. (A) Stu2 mutants used in this study fall into three distinct categories of polymerase activity, as quantified by Geyer *et al.* (2018). Mutations to disrupt  $\alpha\beta$ -tubulin binding in each of the TOG domains, R200A and R519A, are denoted as TOG1\* and TOG2\*, respectively. (B) Representative MT array formation at the Spc110c(T) when wild-type Stu2 (RKY122), Stu2 TOG1\* (RKY126), Stu2 TOG2\* (RKY133), Stu2  $\Delta$ cc 2xbasic (RKY140), Stu2 TOG1\* TOG2\* (RKY132), and Stu2  $\Delta$ cc (RKY139) are expressed.  $\gamma$ -tubulin complexes are visualized with Spc97-mCherry (shown in magenta) and tubulin is visualized with GFP-Tub1 (shown in cyan). Arrows denote SPBs and carets denote ectopically localized  $\gamma$ -tubulin complexes. (C) Cumulative percent of cells over time in which Spc110c(T) forms a MT array over a three-hour period following nocodazole washout. Values are mean  $\pm$  S.D. There were 2 biological replicates for all conditions and 101, 135, 157, 71, 138, and 154 total cells for Stu2, Stu2 TOG1\*, Stu2 TOG2\*, Stu2  $\Delta$ cc 2xbasic, Stu2 TOG1\* TOG2\*, and Stu2  $\Delta$ cc, respectively. (D) Percent of cells in which Spc110c(T) forms a MT array plotted against MT elongation rate, where each is normalized to the activity of wild-type Stu2. Data represents the results of Figure 5C and the published results of Geyer *et al.* (2018). Colors correspond to color of boxes surrounding the depictions of the three classes of mutants in (A).

arrays is the same in control cells as in *vik1* $\Delta$ /*vik1* $\Delta$  cells (Figure 7C). However, in control cells, Spc97-mCherry usually localizes to two bright puncta at the end of ectopic MT arrays

(73% of cells, Figure 7D). In contrast, Spc97-mCherry is more evenly distributed along Spc110c(T)-associated MT arrays in *vik1* $\Delta$ /*vik1* $\Delta$  cells. This phenotype was quantified using the root mean squared error (RMSE) (Equation 1):

$$\text{RMSE} = \sqrt{\frac{1}{n} \sum_{i=1}^n (y_i - \hat{y}_i)^2} \quad (1)$$

where  $n$  = number of Spc110c(T) MT bundles measured,  $y_i$  = Spc97-mCherry intensity at a given point within the bundle, and  $\hat{y}_i$  = mean Spc97-mCherry intensity across the MT bundles. When  $\gamma$ -tubulin complexes cluster, the Spc97-mCherry intensity at any given point will be brighter and thus further from the mean of the Spc97-mCherry intensity along the MT bundle. Using this measure, Vik1 significantly promotes MT minus end clustering ( $P < 0.001$ , Figure 7E).

The Spc110c(T) provides a unique system to analyze the roles of MAPs and motors whose roles have been obscured in the context of the resilient bipolar spindle. Here we report previously undetected roles for Stu2, Bim1, Bik1, Kip3, and Vik1 in the formation of a bipolar MT array in the nucleus.

The formation of a bipolar array at the Spc110c(T) can be divided into a number of steps, beginning with the recruitment of the  $\gamma$ -tubulin complex to the Spc110c(T). Of the MAPs and motors included in this study, we found that none affected the ability of the Spc110c(T) to recruit the  $\gamma$ -tubulin complex. The ability of the Spc110c(T) to recruit might be strictly due to upstream regulation, such as post-translational modifications and/or oligomerization states of the nucleation machinery (Lyon *et al.* 2016).

The Spc110c(T) also revealed previously unreported roles in MT nucleation for Stu2, Bim1, Bik1, and Kip3 in budding yeast nuclei. Bim1 and Kip3 join their homologs as promoters of MT nucleation (Vitre *et al.* 2008; West and McIntosh 2008; Erent *et al.* 2012). Bik1 becomes the first CLIP170 homolog to be implicated in MT nucleation, but due to its role in SPB positioning, the delay in MT formation at the Spc110c(T) may be an indirect consequence of SPB localization. Stu2 is now shown to promote MT nucleation in the nucleus in addition to the cytoplasm (Gunzelmann *et al.* 2018). Further, the polymerase activity of Stu2 *in vitro* correlates well with its nucleation activity *in vivo*, which supports the theory that Stu2 homologs function to elongate nascent MTs during nucleation (King *et al.* 2020).

Finally, we report a role for Vik1 in MT minus end focusing. Kinesin-14 motor proteins have been implicated in spindle repair via MT minus end focusing in other eukaryotic cells (Endow and Komma 1998; Kwon *et al.* 2008; Lecland and Lüders 2014). However, this is the first evidence of this role for Vik1, suggesting a broadly conserved role for the kinesin-14 motor proteins.

## Acknowledgments

We thank Matthew Miller for the plasmids to integrate Stu2 mutants. We thank Luke Rice and Elisabeth Geyer for helpful discussions.

B.R.K. designed and performed research, analyzed the data, and wrote the manuscript. J.B.M. performed tomography experiments. T.V. performed research. M.W. contributed experimental design, supervised research and edited the manuscript. E.G.M. contributed experimental design and edited the manuscript. T.N.D. contributed experimental design, analyzed data, supervised the research, and helped write the manuscript.

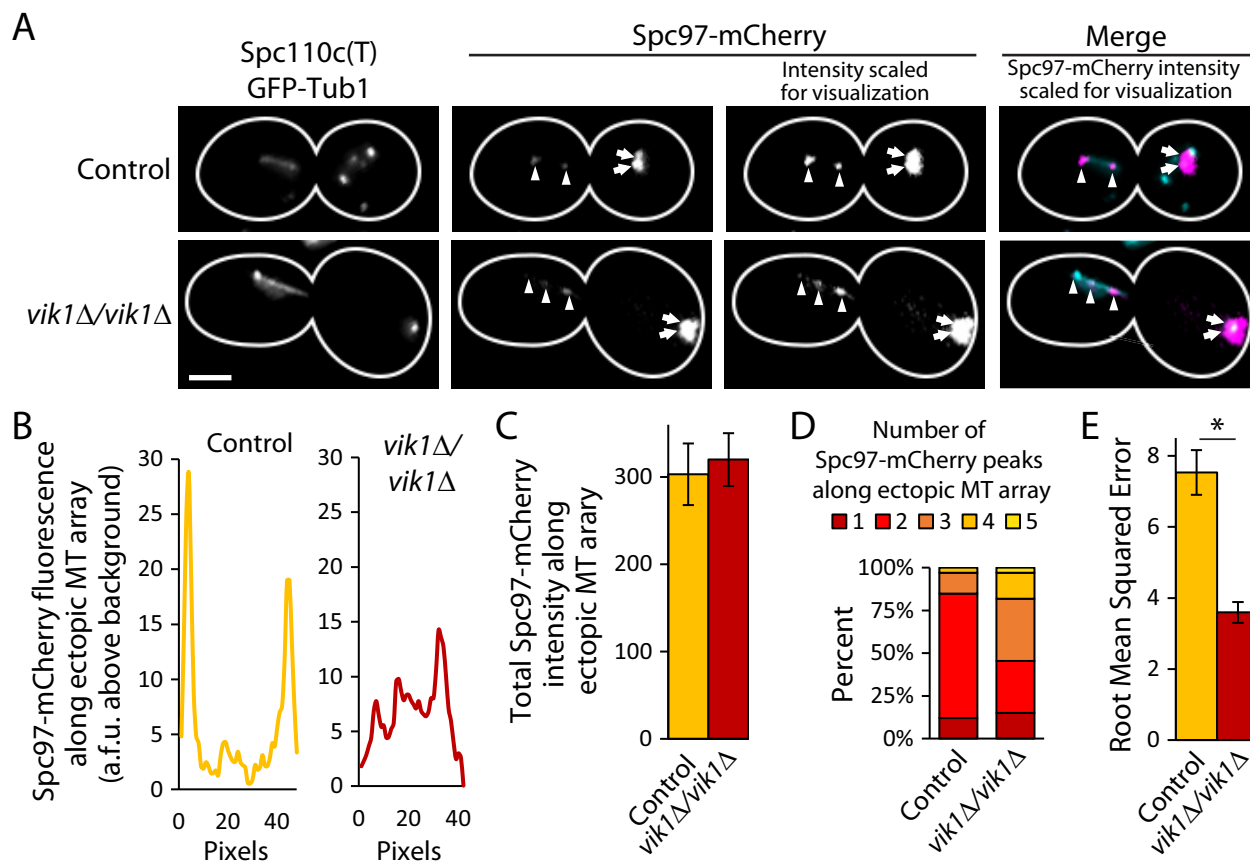


**Figure 7** Vik1 significantly promotes  $\gamma$ -tubulin complex clustering. (A) Representative control (RKY52) shows that the Spc110c(T) characteristically forms MT bundles with distinct  $\gamma$ -tubulin complex puncta at each end (top), and in *vik1Δ/vik1Δ* (RKY31), the Spc110c(T) forms MT arrays with dispersed  $\gamma$ -tubulin complexes along the array. (B) Representative line scan of the average Spc97-mCherry intensity at a given pixel along the length of a 10-pixel wide line scan of the Spc110c(T) associated MT array in control (left) and *vik1Δ/vik1Δ* cells (right). Data plotted is the sum intensity above background fluorescence across a 10-pixel line. (C) Average total Spc97-mCherry intensity along Spc110c(T)-associated MT arrays. (D) Number of Spc97-mCherry peaks along ectopic MT arrays differs between control cells and *vik1Δ/vik1Δ* cells. (E) Average RMSE of Spc97-mCherry distribution along line scans of Spc110c(T)-associated MT bundles. Data plotted are means  $\pm$  S.D. (control  $N = 28$ , *vik1Δ/vik1Δ*  $N = 33$ ). Asterisk denotes significance as measured by t-test,  $P < 0.001$ .

## Funding

This study was supported by grants from the National Institutes of Health grants P01 GM105537 to Mark Winey, R35 GM130293 to Trisha Davis, and T32 GM007270 to Brianna Rose King.

Conflicts of interest: None declared.

## Literature cited

- Blake-Hodek K, Cassimeris L, Huffaker TC. 2010. Regulation of microtubule dynamics by Bim1 and Bik1, the budding yeast members of the EB1 and CLIP-170 families of plus-end tracking proteins. *Mol Biol Cell* 21:2013–2023.
- Brouhard GJ, Stear JH, Noetzel TL, Al-Bassam J, Kinoshita K, et al. 2008. XMAP215 is a processive microtubule polymerase. *Cell* 132:79–88.
- Burke D, Dawson D, Stearns T. 2000. *Methods in Yeast Genetics: A Cold Spring Harbor Laboratory Course Manual*. Cold Spring Harbor, USA: Cold Spring Harbor Laboratory Press.
- Carvalho P, Gupta ML, Hoyt MA, Pellman D. 2004. Cell cycle control of kinesin-mediated transport of Bik1 (CLIP-170) regulates microtubule stability and dynein activation. *Dev Cell* 6:815–829.
- Caudron F, Andrieux A, Job D, Boscheron C. 2008. A new role for kinesin-directed transport of Bik1p (CLIP-170) in *Saccharomyces cerevisiae*. *J Cell Sci* 121:1506–1513.
- Costanzo M, Vandersluis B, Koch EN, Baryshnikova A, Pons C, et al. 2016. A global genetic interaction network maps a wiring diagram of cellular function. *Science* 353:aaf1420.
- Cottingham FR, Gheber L, Miller DL, Hoyt MA. 1999. Novel roles for *Saccharomyces cerevisiae* mitotic spindle motors. *J Cell Biol* 147:335–349.
- Derr ND, Goodman BS, Jungmann R, Leschziner AE, Shih WM, et al. 2012. Tug-of-war in motor protein ensembles revealed with a programmable DNA origami scaffold. *Science* 338:662–665.
- DeZwaan TM, Ellingson E, Pellman D, Roof DM. 1997. Kinesin-related KIP3 of *Saccharomyces cerevisiae* is required for a distinct step in nuclear migration. *J Cell Biol* 138:1023–1040.
- Endow SA, Komma DJ. 1998. Assembly and dynamics of an anastral: astral spindle: the meiosis II spindle of *Drosophila* oocytes. *J Cell Sci* 111:2487–2495.
- Erent M, Drummond DR, Cross RA. 2012. *S. pombe* kinesins-8 promote both nucleation and catastrophe of microtubules. *PLoS One* 7:e30738.
- Fukuda Y, Luchniak A, Murphy ER, Gupta ML. 2014. Spatial control of microtubule length and lifetime by opposing stabilizing and destabilizing functions of kinesin-8. *Curr Biol* 24:1826–1835.
- Furuta K, Furuta A, Toyoshima YY, Amino M, Oiwa K, et al. 2013. Measuring collective transport by defined numbers of processive and nonprocessive kinesin motors. *Proc Natl Acad Sci USA* 110:501–506.

- Gardner MK, Zanic M, Gell C, Bormuth V, Howard J. 2011. Depolymerizing kinesins Kip3 and MCAK shape cellular microtubule architecture by differential control of catastrophe. *Cell*. 147:1092–1103.
- Geiser JR, Schott EJ, Kingsbury TJ, Cole NB, Totis LJ, et al. 1997. *Saccharomyces cerevisiae* genes required in the absence of the CIN8- encoded spindle motor act in functionally diverse mitotic pathways. *Mol Biol Cell*. 8:1035–1050.
- Geyer EA, Miller MP, Brautigam CA, Biggins S, Rice LM. 2018. Design principles of a microtubule polymerase. *eLife*. 7:e34574.
- Gietz RD, Schiestl RH, Willems AR, Woods RA. 1995. Studies on the transformation of intact yeast cells by the LiAc/SS-DNA/PEG procedure. *Yeast*. 11:355–360.
- Greenland KB, Ding H, Costanzo M, Boone C, Davis TN. 2010. Identification of *Saccharomyces cerevisiae* spindle pole body remodeling factors. *PLoS One*. 5:e15426.
- Gunzelmann J, Rütznick D, Lin TC, Zhang W, Neuner A, et al. 2018. The microtubule polymerase Stu2 promotes oligomerization of the  $\gamma$ -TuSC for cytoplasmic microtubule nucleation. *eLife*. 7:e39932
- Gupta ML, Carvalho P, Roof DM, Pellman D. 2006. Plus end-specific depolymerase activity of Kip3, a kinesin-8 protein, explains its role in positioning the yeast mitotic spindle. *Nat Cell Biol*. 9:913–923. 8:
- Hoyt MA, He L, Loo KK, Saunders WS. 1992. Two *Saccharomyces cerevisiae* kinesin-related gene products required for mitotic spindle assembly. *J Cell Biol*. 118:109–120.
- King BR, Moritz M, Kim H, Agard DA, Asbury CL, et al. 2020. XMAP215 and gamma-tubulin additively promote microtubule nucleation in purified solutions. *Mol Biol Cell*. 31:2187–2194. (Accessed: 2021 March 25) 10.1091/mbc.E20-02-0160.
- Kremer JR, Mastronarde DN, McIntosh JR. 1996. Computer visualization of three-dimensional image data using IMOD. *J Struct Biol*. 116:71–76.
- Kwon M, Godinho SA, Chandhok NS, Ganem NJ, Azioune A, et al. 2008. Mechanisms to suppress multipolar divisions in cancer cells with extra centrosomes. *Genes Dev*. 22:2189–2203.
- Lecland N, Lüders J. 2014. The dynamics of microtubule minus ends in the human mitotic spindle. *Nat Cell Biol*. 16:770–778.
- Lyon AS, Morin G, Moritz M, Yabut KCB, Vojnar T, et al. 2016. Higher-order oligomerization of Spc110p drives gamma-tubulin ring complex assembly. *Mol Biol Cell*. 27:2245–2258.
- Manning BD, Barrett JG, Wallace JA, Granok H, Snyder M. 1999. Differential regulation of the Kar3p kinesin-related protein by two associated proteins, Cik1p and Vik1p. *J Cell Biol*. 144:1219–1233.
- Mastronarde DN. 1997. Dual-axis tomography: an approach with alignment methods that preserve resolution. *J Struct Biol*. 120:343–352.
- McIsaac RS, Oakes BL, Wang X, Dummit KA, Botstein D, et al. 2013. Synthetic gene expression perturbation systems with rapid, tunable, single-gene specificity in yeast. *Nucleic Acids Research*. 41:e57–e57.
- McNally FJ. 2013. Mechanisms of spindle positioning. *J Cell Biol*. 200:131–140.
- Melbinger A, Reese L, Frey E. 2012. Microtubule length regulation by molecular motors. *Phys Rev Lett*. 108:258104. (Accessed: 2021 March 25) 10.1103/PhysRevLett.108.258104
- Miller RK, Cheng SC, Rose MD. 2000. Bim1p/Yeb1p mediates the Kar9p-dependent cortical attachment of cytoplasmic microtubules. *Mol Biol Cell*. 11:2949–2959.
- Miller RK, Heller KK, Frisèn L, Wallack DL, Loayza D, et al. 1998. The kinesin-related proteins, Kip2p and Kip3p, function differently in nuclear migration in yeast. *Mol Biol Cell*. 9:2051–2068.
- Muller EGD, Snysman BE, Novik I, Hailey DW, Gestaut DR, et al. 2005. The organization of the core proteins of the yeast spindle pole body. *Mol Biol Cell*. 16:3341–3352.
- Newman JR, Wolf E, Kim PS. 2000. A computationally directed screen identifying interacting coiled coils from *Saccharomyces cerevisiae*. *Proc Natl Acad Sci USA*. 97:13203–13208.
- O'Connell MJ, Meluh PB, Rose MD, Morris NR. 1993. Suppression of the bimC4 mitotic spindle defect by deletion of klpA, a gene encoding a KAR3-related kinesin-like protein in *Aspergillus nidulans*. *J Cell Biol*. 120:153–162.
- Olmsted ZT, Colliver AG, Riehlman TD, Paluh JL. 2014. Kinesin-14 and kinesin-5 antagonistically regulate microtubule nucleation by  $\gamma$ -TuRC in yeast and human cells. *Nat Commun*. 5:15.
- O'Toole ET, Winey M, McIntosh JR, Mastronarde DN. 2002. Electron tomography of yeast cells. *Methods Enzymol*. 351:81–95.
- Page BD, Satterwhite LL, Rose MD, Snyder M. 1994. Localization of the Kar3 kinesin heavy chain-related protein requires the Cik1 interacting protein. *J Cell Biol*. 124:507–519.
- Popov AV, Severin F, Karsenti E. 2002. XMAP215 is required for the microtubule-nucleating activity of centrosomes. *Curr Biol*. 12:1326–1330.
- Reese L, Melbinger A, Frey E. 2011. Crowding of molecular motors determines microtubule depolymerization. *Biophys J*. 101:2190–2200.
- Roof DM, Meluh PB, Rose MD. 1992. Kinesin-related proteins required for assembly of the mitotic spindle. *J Cell Biol*. 118:95–108.
- Saunders W, Lengyel V, Hoyt MA. 1997. Mitotic spindle function in *Saccharomyces cerevisiae* requires a balance between different types of kinesin-related motors. *Mol Biol Cell*. 8:1025–1033.
- Shetty A, Reim NI, Winston F. 2019. Auxin-inducible degron system for depletion of proteins in *Saccharomyces cerevisiae*. *Curr Protoc Mol Biol*. 128:e104.
- Straight AF, Marshall WF, Sedat JW, Murray AW. 1997. Mitosis in living budding yeast: anaphase a but no metaphase plate. *Science*. 277:574–578.
- Su X, Qiu W, Gupta ML, Pereira-Leal JB, Reck-Peterson SL, et al. 2011. Mechanisms underlying the dual-mode regulation of microtubule dynamics by Kip3/Kinesin-8. *Mol Cell*. 43:751–763.
- Thawani A, Kadzik RS, Petry S. 2018. XMAP215 is a microtubule nucleation factor that functions synergistically with the  $\gamma$ -tubulin ring complex. *Nat Cell Biol*. 20:575–585.
- Thomas BJ, Rothstein R. 1989. Elevated recombination rates in transcriptionally active DNA. *Cell*. 56:619–630.
- Tischer C, Brunner D, Dogterom M. 2009. Force- and kinesin-8-dependent effects in the spatial regulation of fission yeast microtubule dynamics. *Mol Syst Biol*. 5:250–250.
- Usui T, Maekawa H, Pereira G, Schiebel E. 2003. The XMAP215 homologue Stu2 at yeast spindle pole bodies regulates microtubule dynamics and anchorage. *EMBO J*. 22:4779–4793.
- Varga V, Helenius J, Tanaka K, Hyman AA, Tanaka TU, et al. 2006. Yeast kinesin-8 depolymerizes microtubules in a length-dependent manner. *Nat Cell Biol*. 8:957–962.
- Vitre B, Coquelle FM, Heichette C, Garnier C, Chrétien D, et al. 2008. EB1 regulates microtubule dynamics and tubulin sheet closure in vitro. *Nat Cell Biol*. 10:415–421.
- Wang Y, Zhang X, Zhang H, Lu Y, Huang H, et al. 2012. Coiled-coil networking shapes cell molecular machinery. *Mol Biol Cell*. 23:3911–3922.
- West RR, McIntosh JR. 2008. Novel interactions of fission yeast kinesin 8 revealed through in vivo expression of truncation alleles. *Cell Motil Cytoskeleton*. 65:626–640.
- Wieczorek M, Bechstedt S, Chaaban S, Brouhard GJ. 2015. Microtubule-associated proteins control the kinetics of microtubule nucleation. *Nat Cell Biol*. 17:907–918.
- Wigge PA, Jensen ON, Holmes S, Soues S, Mann M, et al. 1998. Analysis of the *Saccharomyces cerevisiae* spindle pole by matrix-assisted laser desorption/ionization (MALDI) mass spectrometry. *J Cell Biol*. 141:967–977.